Title
Optimizing CO2–Loaded Aqueous Amine Solutions for Higher Electrocatalytic CO2 Reduction Activity

Journal
Journal of the American Chemical Society, 147(43)

ISSN
0002-7863

Authors
Mir, Qayoom
Banerjee, Avishek
Ihiri, Ferdawss
et al.

Publication Date
2025-10-29

DOI
10.1021/jacs.5c07783

Optimizing CO_2-Loaded Aqueous Amine Solutions for Higher Electrocatalytic CO_2 Reduction Activity

Ab Qayoom Mir[a], Avishek Banerjee[b], Ferdawss Ihiri[c], Shawn Chiu[c], Anastassia N. Alexandrova[c,d], Carlos Morales-Guio[b], Jenny Y. Yang*[a]

[a]Department of Chemistry, University of California, Irvine, Irvine, CA 92697, USA

[b]Department of Chemical and Biomolecular Engineering, University of California, Los Angeles, Los Angeles, California 90095, United States

[c]Department of Chemistry and Biochemistry, University of California, Los Angeles, Los Angeles, California 90095, United States

[d]Department of Materials Science and Engineering, University of California, Los Angeles, Los Angeles, California 90095, United States

Supporting Information Placeholder

ABSTRACT: The activity of aqueous-based carbon dioxide reduction (CO_2R) reactions is often limited by the solubility of CO_2. The addition of amines can increase the total dissolved carbon (TDC) in water through the formation of bicarbonate and carbamate species, which has been used to great effect to capture CO_2 from dilute streams. In this study we explore the effect of 12 primary and secondary amines of varying Brønsted basicity, steric profile, and hydrogen-bonding capabilities on the aqueous CO_2R to CO activity of a molecular Ni(cyclam)Cl_2 catalyst with a Hg electrode. Addition of some of the amines results in greater activity and selectivity for CO production compared to equivalent aqueous solutions without added amines. Under optimal conditions (0.4 M 3-amino-propionitrile), there is an over five-fold increase in current density compared to equivalent conditions with no amine. Interestingly, the increase in activity did not correlate to any single property of the amines. To elucidate the effect of the amine additives on catalysis, we used vapor-liquid equilibrium modeling (VLE), ^{13}C NMR spectroscopy, and computational analysis to determine the carbon speciation of the solutions. These results indicate that for amines without ethylalcohol functionalities, CO_2R activity correlates with carbamate concentration, which is in turn governed by amine basicity and steric effects. However, this correlation does not persist for amines with ethylalcohol functionalities, which can form more stable carbamates through intramolecular-hydrogen bonding. These studies demonstrate that amine additives can enhance aqueous CO_2R activity and selectivity, and describe key amine properties that lead to these higher performance metrics.

Introduction

The electrolytic reduction of carbon dioxide to replace fossil carbon is a highly sought after goal to reduce greenhouse gas emissions and progress towards a circular carbon economy.[1] Electrocatalytic CO_2 reduction (CO_2R) is often limited by the poor solubility of CO_2 in aqueous solvents under mild conditions (0.034 M at pH 7).[2-9] A few strategies have been pursued to resolve this limitation. One approach is to increase the amount of total dissolved carbon (TDC) in the form of bicarbonate and carbonate by operating at more alkaline conditions (1.18 M at pH 14). However, these systems are limited by the slow release of CO_2 at bipolar membranes, requiring large voltages to achieve appreciable current densities.[10, 11] Another approach is to use gas diffusion electrodes, although flooding from the electrolyte due to pressure imbalances and accumulation of bicarbonate and carbonate salts currently limits lifetimes.[7, 12, 13]

In this study, we investigated the use of amines in aqueous reaction solvent to increase the total dissolved carbon (TDC). Aqueous amine solutions can absorb high concentrations of dissolved carbon in the form of bicarbonate, carbonate, and carbamate. As an example, aqueous solutions with 2.5 – 2.6 M amines can achieve TDCs of 3 – 4 M at near neutral pH conditions.[14, 15] The high affinity of CO_2 towards amines, particularly under aqueous conditions, has been leveraged extensively for capturing CO_2 from dilute streams, followed by thermal release of concentrated CO_2.[16-18] There has been increasing interest in integrated CO_2 capture and conversion, which skips the thermal release and CO_2 concentration step by directly reducing CO_2-loaded aqueous amine solutions. An integrated process has the potential to be significantly more energy efficient and less capital intensive.[19-21]

Chart 1. Structure of Ni(cyclam)Cl_2 and amines and their abbreviations.

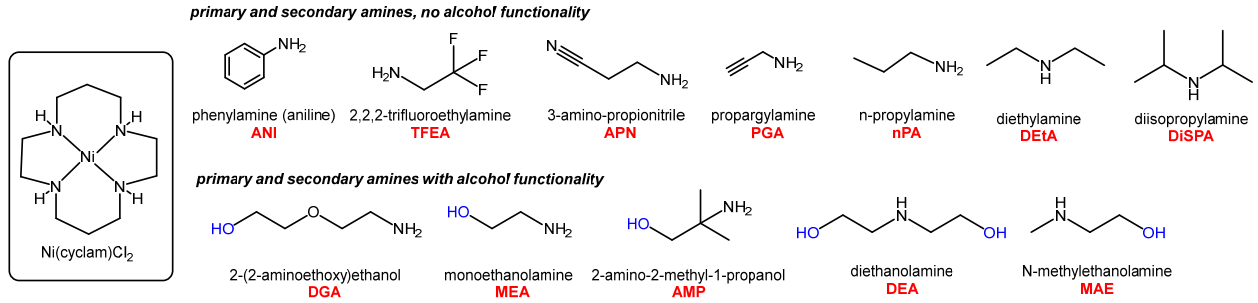

However, there are few examples of using CO_2-amine solutions in electrocatalytic reduction.[22-31] While a few report high Faradaic efficiencies (FE, >85%) for carbon-based products,[31, 32] the addition of amines generally leads to lower FEs compared to the corresponding solution without an amine.[22-30, 33, 34] The loss of selectivity for CO is typically accompanied by higher activity towards the hydrogen evolution reaction (HER).[22-30, 33, 34] Additionally, many of the metallic catalysts suffer from corrosion under reducing potentials, inhibiting activity and reducing overall stability.[23]

To further understand the electrocatalytic reduction of CO_2-loaded aqueous amine solutions, we investigated CO_2R activity with the molecular catalyst Ni(cyclam)Cl_2 (Chart 1) with a Hg electrode. Ni(cyclam)Cl_2 on Hg has previously been studied as an electrocatalyst for the selective reduction of CO_2 to CO.[35-45] We further sought to understand how amine properties such as Brønsted basicity and structure impact CO_2R. Twelve different primary and secondary amines with varying Br∅nsted basicity, steric profiles, and with and without alcohol functionalities were tested (Chart 1). Our results indicate that amine identity plays a significant role in CO_2R activity. Compared to solutions with no added amine, some amines have minimal impact on catalysis while other amines lead to improved current density and selectivity for CO. Notably, we observe no evidence of catalyst poisoning, inhibition, or degradation with any of the amines.

CO_2-loaded aqueous amine solutions contain dissolved CO_2, bicarbonate, carbonate, and carbamate in varying concentrations that all contribute to the total dissolved carbon (TDC). The speciation of these solutions has been shown to impact CO_2R activity for heterogeneous catalysts.[24, 25, 29, 46, 47] The solution speciation is highly dependent on multiple amine properties. To understand the solution composition, vapor-liquid equilibrium (VLE) modeling, theoretical calculations, and ^{13}C NMR spectroscopy were used to understand how speciation impacts catalysis.

Most prior studies on CO_2-loaded aqueous amine solutions have focused on identifying amines that optimize absorption (capture) of CO_2 from dilute streams and facile thermal release of CO_2.[16-18] In this study, we find that different properties are more important for their use in enhancing CO_2R electrocatalysis. Additionally, our correlative study provides information on physical parameters for selecting amine sorbents for the dual purpose of optimizing capture and subsequent electrocatalytic conversion in an integrated process.

Results

Cyclic voltammetry. Cyclic voltammetry (CV) experiments were performed in aqueous solution using a BASi Controlled Growth Mercury Electrode (CGME), which produces hanging mercury (Hg) drop electrode (HMDE) with a reproducible surface area of 0.0384 cm^2.[49, 50] Prior studies with Ni(cyclam)Cl_2 for aqueous CO_2 reduction noted electrocatalytic activity and selectivity for CO was enhanced with Hg working electrodes because it adsorbs onto the Hg surface at cathodic potentials to form the active catalyst.[35, 39-42, 51, 52] Consistent with prior studies,[42] the CV trace of 1 mM Ni(cyclam)Cl_2 in aqueous phosphate buffer (0.05 M) at pH 7 (Figure 1, red trace) did not exhibit any significant reductive features. Addition of 1 atm of CO_2 leads an increase in current at -1.17 V vs Ag/AgCl (sat.), which is attributed to the Ni(II/I) reduction.[42] Prior studies have shown Ni(cyclam)Cl_2 with a Hg working electrode reduces CO_2 to CO with quantitative Faradaic efficiency under acidic conditions (pH ~ 4), with a loss of selectivity for carbon based products at pH 10.6.[41]

The 12 amines selected for study and their abbreviations are shown in Chart 1 and Table 1. Aqueous solutions at pH 7 were prepared with 0.05 M phosphate buffer. Addition of the respective amines to make a 0.1 M solution resulted in an increase in pH to between 7.26 to 11.1 depending on the Brønsted basicity of the amine (see Table S1 for pH values after the addition of each amine). 1 atm of CO_2 was then sparged through the solution for 15 minutes, resulting in a lowering of the pH to 6.1 – 6.8 (Table S1). The solution was then sparged with N_2 for 5 minutes to minimize the amount of free CO_2 in the solution and headspace, leading to final pH values in the range of 6.8 – 8.1, which remained stable over 30 minutes (Table 1 and S1).

Cyclic voltammetry for the CO_2-loaded amine solution with 1 mM Ni(cyclam)Cl_2 and HMDE exhibits an increased current at -1.17 vs Ag/AgCl, the same onset potential observed with CO_2 reduction under aqueous conditions and attributed to the Ni(II/I) reduction. Ni(cyclam)Cl adsorption onto the Hg electrode surface was previously verified by the lack of increase in catalytic current with increasing catalyst concentration.[40] We performed a similar study for CO_2-loaded solutions of the amines monoethanolamine (MEA), 3-amino-propionitrile (APN), or *n*-propylamine (nPA) solution as representatives of the 12 amines, as they span amines of varying pK_{a1} (APN and nPA), and one with

an ethanol functionality (MEA). The catalytic current increased from 0.5 mM to 1 mM of Ni(cyclam)Cl_2, but did not increase at higher concentrations (1.5 and 2 mM), indicating the surface is saturated with the adsorbed species (Figures S2 to S4). All subsequent studies were performed with 1 mM Ni(cyclam)Cl_2. The maximum concentration-independent peak current and surface area of the HMDE (0.0384 cm^2) was used to calculate the total current density (Figure S1, Table S3).

Controlled Potential Electrolysis (CPE). A Hg pool electrode was used for controlled potential electrolysis in an H-cell to determine the products of reduction and the Faradaic efficiency. The amine solutions were prepared using the same method used in the CV experiments. As in the prior CO_2 reduction studies, electrolysis was performed at -1.40 V vs Ag/AgCl (sat.). Representative charge vs time potential traces are shown in Figure S7 and total charge passed listed in Table S2. The headspace was analyzed and products were quantified by gas chromatography (GC); only H_2 and CO were observed. No formate was detected by ^{1}H NMR spectroscopy. Calibration curves for the GC and a representative GC trace from the CPE are shown in Figures S8 and S9, respectively. Equivalent studies on buffered solutions at pH 7 and 8 with no amine were performed to establish baseline activity. Faradaic efficiencies for CO from solutions with no amine at pH 7 and 8 were 44% ± 2.63 and 19% ± 2.07, respectively (Table 1). The lower FE values are consistent with the loss of selectivity and CO production at higher pH values previously described.[41] The Faradaic efficiencies for CO and peak currents in the cyclic voltammetry were used to calculate its partial current density value under the varying conditions, which is shown in Figure 2 for each amine studied. The CO partial current density for ANI, TFEA, and APN are best compared to the pH 7 solution with amine, as their solutions were at pH 6.9, 6.8, and 7.2, respectively (Table 1). PGA and DEtA had an intermediate pH value of 7.5, while the rest of the amines resulted in pH values between 7.7 – 8.1 (Table 1). From this data, the addition of some amines results in increased current densities for CO. However, the activity or selectivity does not correlate directly with the pH of the solution (Figure S10) or amine Brønsted basicity (Figure 2), primary vs secondary amines, or steric effects. To rationalize the trends in CO current density, we investigated the carbon-based speciation in the different amine solutions.

Speciation of CO_2 in aqueous amine solutions. CO_2, H_2O, and amines can all engage in acid-base reactivity. As a result, the speciation of aqueous amine solutions with carbon dioxide can be complex and is strongly dependent on the amine properties, which has been extensively studied because of their importance in CO_2 capture.[16-18, 55-58] In aqueous solution, the two most common initial reactions between amines and CO_2 are shown in eq 1 and 2.[58]

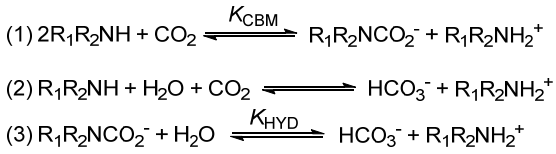

In eq 1, two equivalents of amine react with CO_2 to form the corresponding ammonium carbamate (K_{CBM} in Table 1).[58] Alternatively, sufficiently basic amines can deprotonate water to form hydroxide, which can react with CO_2 to form bicarbonate.[58] The extent of this reactivity is dependent on the amine Brønsted basicity. The reactivity of CO_2 to form carbamate (eq 1) is kinetically favored over the formation of bicarbonate (eq 2).[58-60] However, unstable carbamates

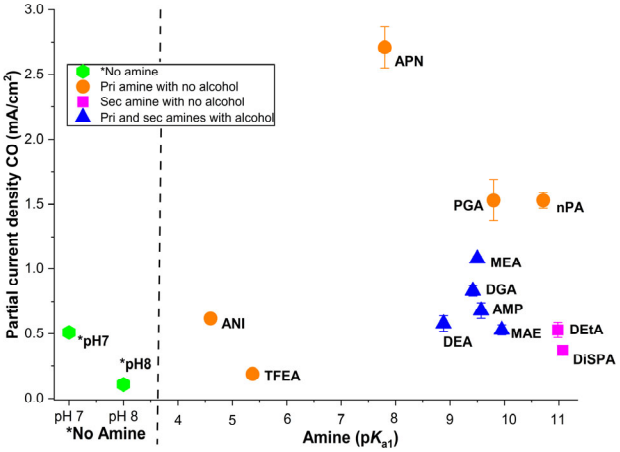

Figure 2. Partial current density for CO for 0.05 M phosphate solutions with no amine at pH 7 and 8 and with 0.1 M amine solutions prepared with CO_2 and N_2 as described in the text with 1 mM Ni(cyclam)Cl_2 on a Hg electrode. Numerical data is listed in Table SX

formed through eq 1 can also hydrolyze (K_{HYD}, eq 3), resulting in the same products as eq 2.[58] Thus, carbamate stability is reflected in both the formation constant (high K_{CBM}, eq 1) and whether it is prone to hydrolysis (low K_{HYD}, eq 3).

At the pH values used in electrolytic studies (6.8 – 8.1), the potential carbon-based species in solution are CO_2 and bicarbonate (HCO_3^-), as well as the respective amine (R_1R_2NH), ammonium ($R_1R_2NH_2^+$), and carbamate ($R_1R_2CO_2^-$) derivatives. Several methods were applied to understand the speciation of these solutions. Vapor-Liquid Equilibrium (VLE) modeling provides the pH-dependent concentrations at varying CO_2 partial pressures, but requires experimentally derived equilibrium constants, which were only available for 7 of the 12 amines studied.[57, 58] To complement the VLE modeling, ^{13}C NMR spectroscopy and computational modeling was also applied. Combined with correlations derived from prior aqueous amine studies, these methods provide a more complete picture of how carbon speciation varies among the different CO_2-loaded aqueous amine solutions.

Vapor-Liquid Equilibrium (VLE) Modeling. The use of well parameterized VLE models have been shown to accurately reproduce product speciation in amine-based aqueous capture of CO_2 applications.[29] The equilibrium species concentration is a function of temperature, pressure, pH, and CO_2 loading. Accurate VLE modeling requires experimentally derived values for K_{CBM} and K_{HYD}, which were only available for ANI,[58] nPA,[58] DEtA,[58] DiSPA,[58] DEA,[58] MEA,[58] and AMP[57] (Table 2). A modified Kent-Eisenberg modeling approach was used to model the chemical speciation of the different primary and secondary amines used in this study. Kent-Eisenberg is the simplest of thermodynamic models as it assumes an ideal gas and solution with all the non-idealities included in the temperature dependent equilibrium constant for the formation of the different species. The modeling approach used has previously been described in the work of Banerjee et al. and further discussion on the development of the model has been included in the SI.[46] The equilibrium constants used for each amine (K_{CBM} and K_{HYD}) in the model and the calculated concentration of the different species along with the total dissolved carbon (TDC) is listed in Table 1.

Computational studies. Two pK_a values are relevant to describe the acid-base properties of the amines, shown in eq 4 and 5.

(4) $R_1R_2NH_2^+ \xrightarrow{pKa_1} R_1R_2NH + H^+$

(5) $R_1R_2NH \xrightarrow{pKa_2} R_1R_2N^- + H^+$

The pK_{a1} value represents the acidity of the protonated amine (ammonium cation), or Brønsted basicity of the amine. pK_{a1} is more easily measured and aqueous values are readily available for most amines from the literature.[56, 62-64] Because the reaction of amines and CO_2 result in the formation of ammonium (eq 1 – 3), pK_{a1} plays an important role in the speciation of aqueous-CO_2 solutions.

The acidity of primary and secondary amines is represented by pK_{a2}. This value is more challenging to measure and few experimental values have been reported. However, pK_{a2} tends to correlate more strongly with calculated CO_2 binding in the absence of steric or other secondary effects.[65] To obtain these values, pK_{a2} for the amines in this study were calculated using density functional theory (DFT) (Table 2 and S4, methods in SI). From our computational results, we find that pK_{a2} values correlate more closely with pK_{CO2} than pK_{a1} as previously described (Figures S22 and S23).[65]

^{13}C NMR Spectroscopy. The aqueous CO_2-amine solutions were also analyzed by ^{13}C NMR spectroscopy. In order to obtain sufficient signal, 1 M amine solutions were used. The solutions were otherwise prepared the same as those used for CV and CPE experiments by purging with CO_2 followed by N_2. ^{13}C NMR spectra were collected from 0.55 mL of amine solutions with additional 0.1 mL of deuterated solvent (D_2O, 99.9%) for locking. A 600 MHz NMR spectrometer with a single pulse program (*zgig*) inverse gated proton decoupled technique was used, with a D1 (delay time) of 15 s and 100 scans.

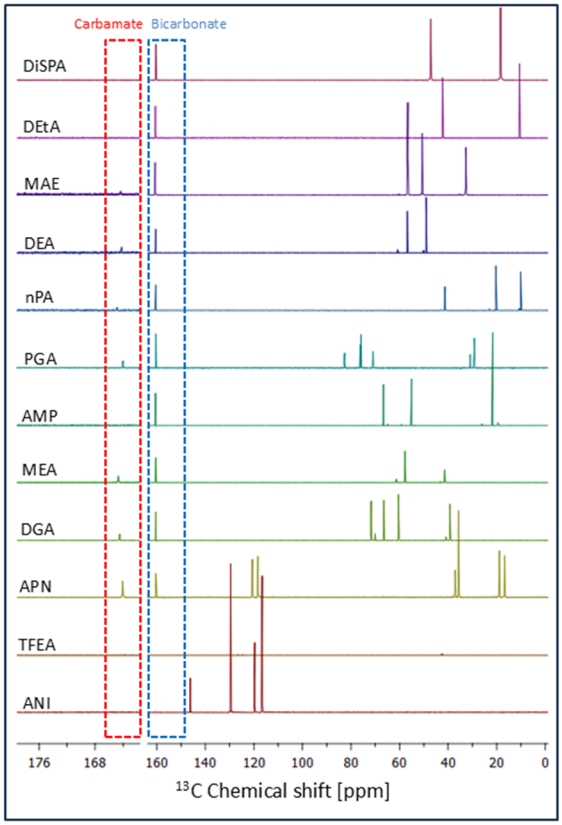

Figure 3. ^{13}C NMR spectra for CO_2-loaded amine solutions. Solutions were prepared by purging 1 M amine solutions with CO_2 for 15 minutes followed by N_2 for 5 minutes. The carbamate region is enclosed in the dashed red box, while the bicarbonate resonance is in the dashed blue box.

While this experimental data is not quantitative,[66] it provides experimental evidence for the presence or absence of carbamate and/or bicarbonate species in solution (Figure 3). This data is consistent with the data obtained using VLE modeling, including the absence of carbamate and bicarbonate in both ANI and TFEA, the absence of carbamate with appreciable bicarbonate with DiSPA and AMP, and the presence of both carbamate and bicarbonate with nPA, DEA, and MEA. The only variance is observed with DEtA. For DEtA, the corresponding carbamate is expected to be present at the lowest concentration of the carbamate forming amines (2.26×10^{-5} M, Table 1). From this data, we assume a lower limit of $\sim 10^{-4}$ M is required for detection of carbamate by ^{13}C NMR spectroscopy under these conditions. Based on this data, we expect the corresponding carbamate concentration for the TFEA solutions is $< 10^{-4}$ M (Table 1).

Discussion

Aqueous amine speciation with CO_2 involves a confluence of properties, including their type (primary versus secondary), basicity, steric properties, and the presence of an alcohol functionality. We did not find direct correlations between CO partial current density and pK_{a1} (Figure 2), pK_{a2}

Table 1. The pH, FE% (CO), and FE%(H_2) is experimental data from this study. Experimental pK_{a1} values are from ref. 42, 47-49. pK_{a2} values were calculated in this study. K_{CBM} and K_{HYD} values are from ref. 44, except for the K_{CBM} for AMP, which is from ref. 58. The greyed boxes indicate these values are not available in the literature. The concentations of carbamate [$R_1R_2NCO_2^-$], bicarbonate [HCO_3^-], and total dissolved carbon were calculated from the VLE model using K_{CBM} and K_{HYD}, and were not determined for amines without these values (grayed out) except for TFEA, where ^{13}C NMR spectroscopy indicate the absence of appreciable amounts of carbamate and bicarbonate.

	Amine	pH	FE% (CO)	FE% (H_2)	pK_{a1} (pK_{a2})	K_{CBM}	K_{HYD}	[$R_1R_2NCO_2^-$]	[HCO_3^-]	[TDC]
Primary Amines Without Alcohol	 phenylamine (aniline) **ANI**	6.9	36±13	40±11	4.6 (27.8)	8.1×10^{-3}	3.6	$<10^{-4}$		
	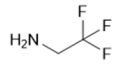 2,2,2-trifluoroethylamine **TFEA**	6.8	11.65±6	102±8.3	5.37 (33.6)			$<10^{-4}$		
	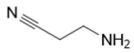 3-amino-propionitrile **APN**	7.2	69.7±17	14±10.75	7.8 (34.4)					
	 propargylamine **PGA**	7.5	61.33±13	3.5±0.89	9.8 (35.1)					
	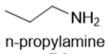 n-propylamine **nPA**	7.8	92.3±7.41	Trace	10.71 (37.6)	1.5×10^{6}	1.3×10^{-2}	9.3×10^{-4}	9.74×10^{-2}	0.102
Secondary Amines Without Alcohol	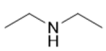 diethylamine **DEtA**	7.7	33 ±7.62	53±12.29	10.98 (35.9)	7.4×10^{4}	2.4×10^{-1}	2.26×10^{-5}	9.94×10^{-2}	0.104
	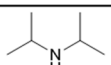 disopropylamine **DiSPA**	8.1	38 ±1.44	66±6.5	11.07 (36.4)	< 1	-	$<10^{-4}$		
Primary & Secondary Amines With Alcohol	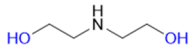 diethanolamine **DEA**	8.0	41 ±10.56	51±15	8.88 (33.6)	2.1×10^{3}	1.5×10^{-1}	1×10^{-3}	9.21×10^{-2}	9.51×10^{-2}
	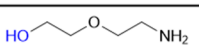 2-(2-aminoethoxy)ethanol **DGA**	7.8	53.5 ±4.17	2.57±1.2	9.42 (36.6)					
	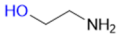 monoethanolamine **MEA**	7.9	77 ±4.15	33±9.7	9.5 (36.5)	6×10^{4}	1.9×10^{-2}	2.2×10^{-3}	9.43×10^{-2}	9.94×10^{-2}
	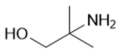 2-amino-2-methyl-1-propanol **AMP**	8.0	61.3±4.23	0.94±.35	9.57 (36.2)	< 1	-	$<10^{-4}$		
	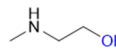 N-methylethanolamine **MAE**	8.1	50.12 ±7.5	34±8.31	9.95 (34.7)					

(Figure S11). For amines in which data is available, we also did not find correlations between the concentration of carbamate (Figure S12), bicarbonate (Figure S13), or total dissolved carbon (TDC, Figure S14). We rationalize the trends in CO partial current density by comparing 1) aliphatic primary amines of varying pK_a and minimal steric interactions, 2) secondary amines of varying steric sizes,

and 3) primary and secondary amines with ethylalcohol functionalities and their speciation.

Primary Amines without Ethylalcohol Functionalities. To characterize the impact of the Brønsted basicity of the amine (pK_{a1}), we first considered primary amines with minimal steric effects and without ethanol functionalities (ANI, TFEA, APN, PGA, and nPA), which are shown as orange circles in Figure 2. Both steric effects and ethanol functionalities are known to impact carbamate formation (*vide infra*).

Amines with pK_{a1} values below 6 are insufficiently basic to either form carbamate (eq 1) or deprotonate water to capture CO_2 as bicarbonate (eq 2).[56] As a result, aniline (ANI) and TFEA, with a pK_{a1} values of 4.6 and 5.37, respectively, are not expected to have significant impacts on CO_2 absorption or speciation. (ANI has a reported K_{CBM} = 8.1 x 10^{-3}, Table 1, indicating minimal carbamate formation).[58] Consistent with this expectation, there is no signal for either carbamate or bicarbonate species in the ^{13}C NMR spectra (Figure 3) for the CO_2-loaded ANI or TFEA solutions. Thus, these amines have minimal impact on CO_2 absorption and total dissolved carbon (TDC). Our experimental data shows that the CO_2-loaded ANI solution (pH = 6.9) has comparable selectivity and current density compared to the pH 7 solution without an amine. The CO_2-loaded TFEA solution (pH = 6.8) exhibits higher activity towards the hydrogen evolution reaction (HER) and correspondingly lower activity and selectivity for CO compared to the ANI solution and pH 7 solution without an amine (Table S2). The source of the higher HER with TFEA difference is not clear; it may be that TFEA may have other properties that favor hydrogen evolution. Neither solution demonstrates any significant enhanced current density or selectivity towards CO production compared to the aqueous solutions at a similar pH of 7 without an amine present.

Prior work on aqueous amine-based CO_2 capture has shown that in the absence of steric effects or hydrogen-bonding functionalities, carbamate formation is primarily dependent on the amine basicity (pK_{a1}). For amines with a pK_{a1} above 6, we expect the formation of carbamate to increase with amine Brønsted basicity until equation 2 becomes more favorable, which occurs at a pK_{a1} of about 9.[56] Although a K_{CYB} has not been measured for APN (pK_{a1} = 7.8), the pH-dependent concentration of its carbamate was quantified by Gallant and co-workers by NMR spectroscopy.[29] They found that the concentration of the carbamate species reaches a maximum around pH 7.2, the pH at which our experiments are performed, with a concentration of ~0.8 M carbamate with ~0.3 M HCO_3^-.[29] We note that because their measurements were made under different conditions (1 atm CO_2), the concentration of carbamate and bicarbonate are likely lower in our solutions. However, APN is expected to have the highest concentration of carbamate of any of these amines because it is close to the ideal pK_{a1} (7 – 8) for carbamate formation. As the pK_{a1} increases for PGA and nPA, the concentration of carbamate also decreases while more of the TDC is in the form of bicarbonate, although both species remain present (Figure 3). Because the latter effect is quantitatively larger, the TDC increases with more basic amines.[46] This trend in speciation is confirmed by the VLE modeling (Figure S21 and Table 1). A decreasing carbamate concentration coupled with increasing bicarbonate concentration was also experimentally confirmed by Gallant and co-workers when comparing APN and n-butylamine (nBA).[29] Although n-BA was not used in this study, it has a similar pK_a (10.8) and steric profile compared to n-propylamine (nPA 10.71) used herein. Thus, the highest CO_2R activity is found with the amine that generates the highest concentration of carbamate, APN.

The use of all three primary amines, APN, PGA, and nPA, results in greater activity and selectivity for CO compared to aqueous solutions with no amine. The partial current density for CO does not correlate with the TDC, but instead is the highest for the solution with the highest concentration of carbamate (APN), while decreasing for PGA and nPA. However, the selectivity for CO improves with more basic amines (higher pK_{a1}) with no H_2 detected with nPA. The protonated ammonium cations are present in solution under these conditions, and could potentially serve as facile proton donors for HER. Although the pH of the solutions is similar, we believe the more basic ammoniums may suppress HER, leading to higher selectivity for CO.

From these results, there is a relationship between amine Brønsted basicity with overall CO_2R activity for CO using the primary amines ANI, TFEA, APN, PGA, and nPA. The amines with lower pK_{a1} values, ANI and TFEA, do not form carbamate or bicarbonate in appreciate concentrations and their CO_2R activity is comparable or lower than solutions with no amine added. APN has both the highest activity and highest concentration of carbamate. The carbamate concentration then decreases with the amines with higher pK_{a1} values, leading to lower activity for CO_2R as more of the TDC is present as bicarbonate.

Secondary Amines Without Ethylalcohol Functionalities. Two secondary amines without ethylalcohol functionalities were also tested (DEtA and DiSPA). Secondary amines are known to generate carbamates with lower relative stability compared to unhindered primary amines of similar Brønsted basicity due to their larger steric properties.[56]

A good illustration of this effect is the comparison of primary amine nPA and secondary amine DEtA. Both have alkyl functionalities that minimize steric effects and similar pK_{a1} values (10.71 for nPA and 10.98 for DEtA). nPA has a significantly higher carbamate formation constant compared to DEtA, with K_{CBM} of $1.5x10^6$ vs $7.4x10^4$, respectively (Table 2). nPA also has a lower hydrolysis constant compared to DEtA (K_{HYD} of $1.3x10^{-2}$ vs $2.4x10^{-1}$, respectively), indicating greater stability towards hydrolysis. These differences are evident in the VLE data,

where nPA has a carbamate concentration of 9.2 x 10^{-4} M vs 2.26 x 10^{-5} for DEtA. In our catalytic studies, DEtA exhibits about half the partial current density for CO compared to nPA, similar to solutions with no amine, which we attribute to the lower concentration of carbamate for DEtA due to the increased steric pressure in the latter.

To further explore the impact of carbamate concentration, we also tested DiSPA, which is only slightly more basic than DEtA (pK_{a1} of 11.07 versus 10.98). However, DiSPA is even more sterically hindered, resulting in no appreciable carbamate formation upon addition of CO_2 (K_{CBM} < 1 with negligible carbamate formation).[58] The partial current density DiSPA for CO is about half of what is observed for DEtA. Thus, for the three amines with similar pK_{a1} values but decreasing carbamate formation due to steric effects, nPa, DEtA, and DiSPA, we see the partial current density again trend with carbamate concentration. The selectivity for CO in this series is also lower than the primary amines without ethylalcohol functionalities. The lower selectivity compared to nPA, which has a similar pK_{a1} value, may relate to the lower carbamate concentrations in DEtA and DiSPA. However, it is difficult to draw firm conclusions as the correlation is less robust.

Amines with Ethylalcohol Functionalities.

Five amines with alcohol functionalities were studied, including three primary amines (DGA, MEA, and AMP) and two secondary amines (DEA and MAE). These derivatives did not follow the same correlation between carbamate concentration and CO partial current density as the amines without ethylalcohol functionalities discussed above, and are thus discussed separately.

MEA is one of the most heavily studied amines in CO_2 capture because it has a high propensity for carbamate formation. Among the amines with reported K_{CBM} values, it is expected, along with DEA, to form the highest concentration of carbamate based on the VLE modeling. Only APN, which does not have reported K_{CBM} values, was shown experimentally to have higher concentrations of carbamate than MEA at these pH values.[29] Despite the fact that MEA and DEA have higher carbamate concentrations (2.2 x 10^{-3} M and 1.0 x 10^{-3} M, respectively) compared to nPa (9.3 x 10^{-4} M) and DEtA (2.26 x 10^{-5} M), it has a lower current density for CO. Thus, these amines with ethylalcohol functionalities are less active for CO_2R to CO despite having higher carbamate concentrations compared to similar alkylamines.

In this group of amines, aminomethylpropanol (AMP) is unusual because it is a primary amine with significant steric hinderance due to the dimethylfunctionalities on the α-carbon. Like DiSPA, the steric properties of AMP inhibit the formation of the corresponding carbamate, leading to a K_{CBM} of < 1 (Table 1), or negligible carbamate concentrations.[57, 61, 67, 68] Thus, the TDC of these solutions will be predominantly bicarbonate (~4 M at pH 7.5),[61] which is corroborated by the VLE analysis (Table 1 and Figure S11) and ^{13}C NMR spectroscopic studies (Figure 3).

As noted with their higher carbamate concentrations, amines functionalized with ethylalcohol groups typically exhibit higher CO_2 uptake compared to their non-functionalized counterparts. Computational and experimental studies indicate that alcohols can stabilize the respective carbamate through an intramolecular hydrogen-bonding interaction, with the greatest stabilization by ethylalcohol functionalities.[69-73] A computational analysis was performed with the amines in this study to quantify this effect. The results indicate intramolecular hydrogen-bonding interactions with the alcohol can lead to stabilization of the carbamate compared to the linear

Table 2. Structures of the corresponding carbamates from DGA, MEA, DEA, and MAE used for calculating free energies in the linear form and cyclic form. The cyclic forms have lower free energies due to intramolecular hydrogen-bonding between the ethanol functionality and the carbamate. The difference in free energy between the linear and cyclic form, or stabilization energy, is given in kcal/mol. Carbon (grey), hydrogen (white), nitrogen (blue), oxygen (red).

Parent Amine	**DGA**	**MEA**	**DEA**	**MAE**
Linear carbamate				
Cyclic carbamate	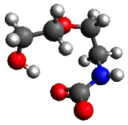	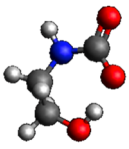	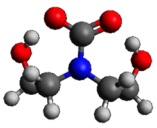	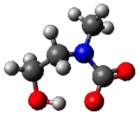
Net stabilization energy of cyclic form	3.72 kcal/mol	5.08 kcal/mol	9.49 kcal/mol	5.24 kcal/mol

conformation (Table 2). The carbamates from four amines (DGA, MEA, DEA, and MAE) were computationally investigated. AMP was not studied as it does not form a stable carbamate with CO_2. The results indicate that for these four amines, the cyclic form with an intramolecular-bond is more stable than the linear form, with DEA the most stabilized (9.49 kcal/mol), followed by MAE (5.24 kcal/mol), MEA (5.08 kcal/mol), and DGA (3.72 kcal/mol).

We believe that for amines with alcohol functionalities, with the exception of AMP which does not form a carbamate, the intramolecular hydrogen-bonding to the carbamate limits the reactivity of the latter. Thus, despite higher carbamate concentrations, their activity is lower than expected compared to their unfunctionalized counterparts. It is unclear from our studies whether carbamate is directly reduced or serving as a buffer for free CO_2. In either scenario, stabilization of the carbamate would lead to the lower activity shown by experiment.

Speciation and CO_2R Activity.

By comparing the CO2R activity from the solutions with and without amines (Figure 2), it is apparent that addition of certain amines can enhance overall activity and selectivity for CO. However, their effects vary greatly depending on the identity of the amine.

From the data we have collected from these 12 amines, we have drawn some correlations about CO_2 speciation and CO_2R activity. Based on the aggregate data, the overall activity does not correlate with total dissolved carbon (TDC) or bicarbonate concentration. For primary and secondary amines without ethylalcohol functionalities, the CO_2R activity correlates with carbamate formation. Carbamate formation requires a minimum Brønsted basicity (pK_{a1} > 6). When minimal steric interactions are present, as they are for ANI, TFEA, APN, PGA, and nPA, carbamate formation increases with pK_{a1} values above 6 until it is above 9, at which deprotonation of water becomes a larger factor The latter tilts the speciation towards bicarbonate over carbamate. The two competing effects are evident in the partial current density for CO, which reaches a maximum with APN for our set of amines with a pK_{a1} of 7.8, and also has the highest carbamate concentration.

Steric interactions result in lower concentrations of carbamate. For sufficiently basic amines, steric effects also result in greater speciation towards bicarbonate and higher TDC values. A good illustration of this effect is shown with nPA, DEtA, and DiSPA, which all have similar pK_{a1} values (10.71, 10.98, and 11.07, respectively) but decrease in carbamate concentration across the series due to their increasing steric interactions. The partial current density for CO trends accordingly, with decreasing values from nPA, DEtA, and DiSPA.

Lastly, amines with ethylalcohol functionalities do not follow the trend of CO_2R activity correlating to carbamate concentration. These amines tend to generate a higher concentration of carbamate compared to unfunctionalized amines with similar pK_{a1}. Despite higher carbamate concentrations, the overall activity with these amines is lower. We hypothesize this divergent behavior is due to stabilization of the carbamate through intramolecular hydrogen-bonding with the ethylalcohol functionality. Our free energy calculations comparing the linear carbamate and its cyclic, hydrogen-bonded isomer show that this interaction can stabilize the carbamate by 3.72 (DGA) up to 9.49 (DEA) kcal/mol.

For the amines that lead to an increased CO current density, it is challenging to determine the exact source of increased activity. Either CO_2, HCO_3^-, or the carbamate could be reduced and it is not facile to experimentally determine which species is the substrate as they are in equilibrium with each other. One possibility is that the HCO_3^- or the carbamate could be serving as buffers for CO_2. The experimental evidence suggests that HCO_3^- is not a carbon source for catalysis, either through direct reduction or as a buffer, as CO_2R activity does not depend on its concentration. Other studies with this catalyst noted that higher pH conditions led to a loss of activity and selectivity for CO,[41] which is consistent with our conclusion that HCO_3^- is not a carbon source. Most studies interrogating the use of amines for CO_2 capture indicate that carbamates are unlikely to be the species being reduced.[29, 34, 46, 47] Carbamate is also expected to be more challenging to reduce because of the enthalpy associated with forming the N-C bond. CO_2 activation at Ni(cyclam)$^+$ is also expected to occur through a Ni-C interaction to form CO,[37, 38, 40, 74, 75] which is not possible with a carbamate species. For these reasons, we believe the carbamate is not the substrate. However, the equilibrium between ammonium carbamate derivatives and CO_2 is achieved much faster than that between bicarbonate and CO_2.[59, 60] Thus, it can serve as an effective

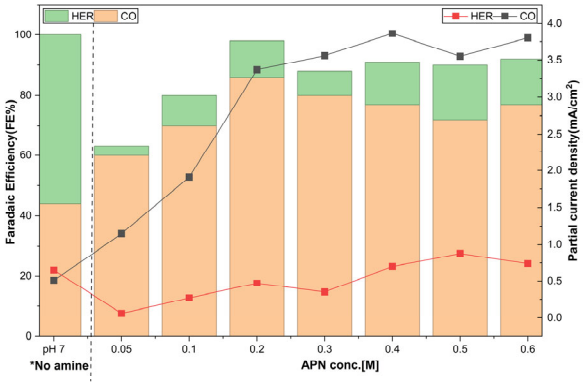

Figure 4: Faradaic efficiencies for CO (orange) and H_2 (green) are shown with the left y-axis at varying concentrations of 2-amino-propionitrile (APN). The corresponding partial current density for CO (black squares) and H_2 (red squares) is shown with the right y-axis. The numerical data with APN is in Table S4 and at pH 7 with no amine in Table S2.

buffer to increase the amount of available CO_2 in solution. This possibility would explain the beneficial effect that amines have on CO_2R activity and the activity correlation with carbamate concentration for the non-ethylalcohol functionalized amines. For the ethylalcohol functionalized amines the intramolecular hydrogen-bond stabilization, which results in increased carbamate concentrations, may also reduce its effectiveness as buffer by slowing down its equilibria with free CO_2.

APN demonstrated the highest activity among all of the amines under our standardized 0.1 M conditions. If the amine is enhancing activity by serving as a buffer with rapid equilibria for dissolved CO_2, higher concentrations could lead to greater activity. We tested the correlation between CO_2R activity and concentration of APN. The current density for CO increases to ~3.5 mA/cm^2 at 0.4 M APN compared to 2 mA/cm^2 at 0.1 M (Figure 4) while maintaining >80% FE for CO. The current does not increase significantly over 0.4 M up to 0.7 M APN.

Conclusions

This study investigated the impact of 12 different amines on the reduction of CO_2-loaded aqueous solutions by Ni(cyclam)Cl_2 with an Hg electrode, with some amines resulting in greater CO_2R *activity* and *selectivity* to CO compared to equivalent solutions without amines present.

Interestingly, the increase in CO_2R activity did not correspond to any single property of the amines. The use of VLE modeling, computational analysis, and ^{13}C NMR spectroscopy was used to identify the important amine properties for enhanced activity. From our analysis, it appears that carbamate formation without secondary interactions is the most important descriptor for CO reduction activity. Thus, activity is optimized for primary amines without steric interactions or hydrogen-bonding functionalities with optimal pK_{a1} values to favor carbamate formation. In our study, this optimal amine corresponded to 3-amino-propionitrile. With 0.4 M APN, the current density for CO production is increased by at least 5-fold with a Faradaic efficiency for CO of >80% compared to equivalent conditions ~44% without amine.

These results are important as they demonstrate amines can be used to increase CO_2R activity in water, which is often restricted by the limited solubility for CO_2. Additionally, the amine properties that are important for CO_2R do not align uniformly with those used to select amines for CO_2 capture and thermal release. The area of integrated CO_2 capture and conversion is rapidly growing. Amines are the most heavily studied liquid-phase sorbent for CO_2 capture. Thus, our conclusions will guide selection of optimal amines for both capture and subsequent catalytic conversion.

ASSOCIATED CONTENT

Supporting Information

Experimental details and methods, Faradaic efficiency calculations, gas chromatography calibrations and related experimental data, cyclic voltammetry and controlled potential electrolysis data, computational methods and full results, vapor-liquid equilibrium modeling results. The Supporting Information is available free of charge on the ACS Publications website.

AUTHOR INFORMATION

Corresponding Author

*j.yang@uci.edu

ACKNOWLEDGMENT

This work was supported as part of the Center for Closing the Carbon Cycle, an Energy Frontier Research Center funded by the U.S. Department of Energy, Office of Science, Basic Energy Sciences under Award Number DE-SC0023427. We are thankful to the UCI Mass Spectrometry Facility for assistance with gas chromatography measurements on Thermo-scientific TRACE 1600 Instrument.

REFERENCES

(1) Shaw, W. J.; Kidder, M. K.; Bare, S. R.; Delferro, M.; Morris, J. R.; Toma, F. M.; Senanayake, S. D.; Autrey, T.; Biddinger, E. J.; Boettcher, S.; et al. A US perspective on closing the carbon cycle to defossilize difficult-to-electrify segments of our economy. *Nature Reviews Chemistry* **2024**, *8* (5), 376-400. DOI: 10.1038/s41570-024-00587-1.

(2) Cheng, W.-H.; Richter, M. H.; Sullivan, I.; Larson, D. M.; Xiang, C.; Brunschwig, B. S.; Atwater, H. A. CO2 Reduction to CO with 19% Efficiency in a Solar-Driven Gas Diffusion Electrode Flow Cell under Outdoor Solar Illumination. *ACS Energy Letters* **2020**, *5* (2), 470-476. DOI: 10.1021/acsenergylett.9b02576.

(3) Chen, Y.; Lewis, N. S.; Xiang, C. Operational constraints and strategies for systems to effect the sustainable, solar-driven reduction of atmospheric CO2. *Energy & Environmental Science* **2015**, *8* (12), 3663-3674, 10.1039/C5EE02908B. DOI: 10.1039/C5EE02908B.

(4) Nitopi, S.; Bertheussen, E.; Scott, S. B.; Liu, X.; Engstfeld, A. K.; Horch, S.; Seger, B.; Stephens, I. E. L.; Chan, K.; Hahn, C.; et al. Progress and Perspectives of Electrochemical CO2 Reduction on Copper in Aqueous Electrolyte. *Chemical Reviews* **2019**, *119* (12), 7610-7672. DOI: 10.1021/acs.chemrev.8b00705.

(5) Singh, M. R.; Clark, E. L.; Bell, A. T. Effects of electrolyte, catalyst, and membrane composition and operating conditions on the performance of solar-driven electrochemical reduction of carbon dioxide. *Phys. Chem. Chem. Phys.* **2015**, *17* (29), 18924-18936, 10.1039/C5CP03283K. DOI: 10.1039/C5CP03283K.

(6) Garg, S.; Li, M.; Weber, A. Z.; Ge, L.; Li, L.; Rudolph, V.; Wang, G.; Rufford, T. E. Advances and challenges in electrochemical CO2 reduction processes: an engineering and design perspective looking beyond new catalyst materials. *Journal of Materials Chemistry A* **2020**, *8* (4), 1511-1544, 10.1039/C9TA13298H. DOI: 10.1039/C9TA13298H.

(7) Higgins, D.; Hahn, C.; Xiang, C.; Jaramillo, T. F.; Weber, A. Z. Gas-Diffusion Electrodes for Carbon Dioxide Reduction: A New Paradigm. *ACS Energy Letters* **2019**, *4* (1), 317-324. DOI: 10.1021/acsenergylett.8b02035.

(8) Sarma, S. C.; Barrio, J.; Bagger, A.; Pedersen, A.; Gong, M.; Luo, H.; Wang, M.; Favero, S.; Zhao, C.-X.; Zhang, Q.; et al.

Reaching the Fundamental Limitation in CO2 Reduction to CO with Single Atom Catalysts. *Adv. Funct. Mater.* **2023**, *33* (41), 2302468. DOI: https://doi.org/10.1002/adfm.202302468.
(9) König, M.; Vaes, J.; Klemm, E.; Pant, D. Solvents and Supporting Electrolytes in the Electrocatalytic Reduction of CO₂. *iScience* **2019**, *19*, 135-160. DOI: 10.1016/j.isci.2019.07.014 (acccessed 2025/08/09).
(10) Badreldin, A.; Li, Y. A critical appraisal of advances in integrated CO2 capture and electrochemical conversion. *Chemical Science* **2025**, *16* (6), 2483-2513, 10.1039/D4SC06642A. DOI: 10.1039/D4SC06642A.
(11) Pimlott, D. J. D.; Kim, Y.; Berlinguette, C. P. Reactive Carbon Capture Enables CO2 Electrolysis with Liquid Feedstocks. *Acc. Chem. Res.* **2024**, *57* (7), 1007-1018. DOI: 10.1021/acs.accounts.3c00571.
(12) Lees, E. W.; Mowbray, B. A. W.; Parlane, F. G. L.; Berlinguette, C. P. Gas diffusion electrodes and membranes for CO2 reduction electrolysers. *Nature Reviews Materials* **2022**, *7* (1), 55-64. DOI: 10.1038/s41578-021-00356-2.
(13) Liu, K.; Smith, W. A.; Burdyny, T. Introductory Guide to Assembling and Operating Gas Diffusion Electrodes for Electrochemical CO2 Reduction. *ACS Energy Letters* **2019**, *4* (3), 639-643. DOI: 10.1021/acsenergylett.9b00137.
(14) Singh, P.; Brilman, D. W. F.; Groeneveld, M. J. Evaluation of CO2 solubility in potential aqueous amine-based solvents at low CO2 partial pressure. *International Journal of Greenhouse Gas Control* **2011**, *5* (1), 61-68. DOI: https://doi.org/10.1016/j.ijggc.2010.06.009.
(15) Jerng, S. E.; Gallant, B. M. Electrochemical reduction of CO2 in the captured state using aqueous or nonaqueous amines. *iScience* **2022**, *25* (7), 104558. DOI: https://doi.org/10.1016/j.isci.2022.104558.
(16) Dutcher, B.; Fan, M.; Russell, A. G. Amine-Based CO2 Capture Technology Development from the Beginning of 2013—A Review. *ACS Applied Materials & Interfaces* **2015**, *7* (4), 2137-2148. DOI: 10.1021/am507465f.
(17) Aghel, B.; Janati, S.; Wongwises, S.; Shadloo, M. S. Review on CO2 capture by blended amine solutions. *International Journal of Greenhouse Gas Control* **2022**, *119*, 103715. DOI: https://doi.org/10.1016/j.ijggc.2022.103715.
(18) Meng, F.; Meng, Y.; Ju, T.; Han, S.; Lin, L.; Jiang, J. Research progress of aqueous amine solution for CO2 capture: A review. *Renewable and Sustainable Energy Reviews* **2022**, *168*, 112902. DOI: https://doi.org/10.1016/j.rser.2022.112902.
(19) Freyman, M. C.; Huang, Z.; Ravikumar, D.; Duoss, E. B.; Li, Y.; Baker, S. E.; Pang, S. H.; Schaidle, J. A. Reactive CO2 capture: A path forward for process integration in carbon management. *Joule* **2023**, *7* (4), 631-651. DOI: https://doi.org/10.1016/j.joule.2023.03.013.
(20) Siegel, R. E.; Pattanayak, S.; Berben, L. A. Reactive Capture of CO2: Opportunities and Challenges. *ACS Catalysis* **2023**, *13* (1), 766-784. DOI: 10.1021/acscatal.2c05019.
(21) Appel, A. M.; Yang, J. Y. Maximum and Comparative Efficiency Calculations for Integrated Capture and Electrochemical Conversion of CO2. *ACS Energy Letters* **2024**, *9* (2), 768-770. DOI: 10.1021/acsenergylett.3c02489.
(22) Neves-Garcia, T.; Hasan, M.; Zhu, Q.; Li, J.; Jiang, Z.; Liang, Y.; Wang, H.; Rossi, L. M.; Warburton, R. E.; Baker, L. R. Integrated Carbon Dioxide Capture by Amines and Conversion to Methane on Single-Atom Nickel Catalysts. *J. Am. Chem. Soc.* **2024**, *146* (46), 31633-31646. DOI: 10.1021/jacs.4c09744.
(23) Choi, J.; Chiu, S.; Banerjee, A.; Sacci, R. L.; Veith, G. M.; Stieber, C.; Hahn, C.; Alexandrova, A. N.; Morales-Guio, C. G. Corrosion and Enhanced Hydrogen Evolution in Electrochemical Reduction of Ammonium Carbamate on Transition Metal Surfaces. *The Journal of Physical Chemistry Letters* **2024**, *15* (31), 8007-8017. DOI: 10.1021/acs.jpclett.4c01638.
(24) Dai, R.; Zhang, L.; Viet Bao Tran, K.; Sirisomboonchai, S.; Machida, H.; Norinaga, K. Mechanism investigation of direct electrochemical reduction of CO2-loaded 2-(ethylamino)ethanol solution into CO. *Sep. Purif. Technol.* **2025**, *355*, 129575. DOI: https://doi.org/10.1016/j.seppur.2024.129575.
(25) Bruggeman, D. F.; Rothenberg, G.; Garcia, A. C. Investigating proton shuttling and electrochemical mechanisms of amines in integrated CO2 capture and utilization. *Nature Communications* **2024**, *15* (1), 9207. DOI: 10.1038/s41467-024-53543-4.
(26) Xiao, Y. C.; Sun, S. S.; Zhao, Y.; Miao, R. K.; Fan, M.; Lee, G.; Chen, Y.; Gabardo, C. M.; Yu, Y.; Qiu, C.; et al. Reactive capture of CO2 via amino acid. *Nature Communications* **2024**, *15* (1), 7849. DOI: 10.1038/s41467-024-51908-3.
(27) Bohlen, B.; Daems, N.; Su, Z.; Chen, A.; Lipkowski, J.; Breugelmans, T. In Situ Spectroelectrochemical Study of Acetate Formation by CO2 Reduction Using Bi Catalyst in Amine-Based Capture Solution. *ChemSusChem* **2024**, *17* (20), e202400437. DOI: https://doi.org/10.1002/cssc.202400437.
(28) Li, Q.; Qu, T.; Tan, S.; Wang, T.; Ding, Y.; Wang, C.; Zhang, J.; Xiong, Z.; Zhao, Y. Structure–activity relationship of a dual-function amine-based electrolyte for integrated CO2 capture and electrochemical conversion. *Chemical Engineering Journal* **2024**, *498*, 155056. DOI: https://doi.org/10.1016/j.cej.2024.155056.
(29) Leverick, G.; Bernhardt, E. M.; Ismail, A. I.; Law, J. H.; Arifutzzaman, A.; Aroua, M. K.; Gallant, B. M. Uncovering the Active Species in Amine-Mediated CO2 Reduction to CO on Ag. *ACS Catalysis* **2023**, *13* (18), 12322-12337. DOI: 10.1021/acscatal.3c02500.
(30) Lee, G.; Li, Y. C.; Kim, J.-Y.; Peng, T.; Nam, D.-H.; Sedighian Rasouli, A.; Li, F.; Luo, M.; Ip, A. H.; Joo, Y.-C.; et al. Electrochemical upgrade of CO2 from amine capture solution. *Nature Energy* **2021**, *6* (1), 46-53. DOI: 10.1038/s41560-020-00735-z.
(31) Siegel, R. E.; Aceves, M.; Berben, L. A. Direct Electrochemical Conversion of CO2 Sorbent Solution to Formate by a Molecular Iron Catalyst. *ACS Energy Letters* **2024**, *9* (6), 2896-2901. DOI: 10.1021/acsenergylett.4c00901.
(32) Verma, P. K.; McCrory, C. C. L. The influence of exogenous amines on the electrochemical CO2 reduction activity of a cobalt–pyridyldiimine catalyst. *Chemical Communications* **2024**, *60* (62), 8039-8042, 10.1039/D4CC02709D. DOI: 10.1039/D4CC02709D.
(33) Bhattacharya, M.; Sebghati, S.; VanderLinden, R. T.; Saouma, C. T. Toward Combined Carbon Capture and Recycling: Addition of an Amine Alters Product Selectivity from CO to Formic Acid in Manganese Catalyzed Reduction of CO2. *J. Am. Chem. Soc.* **2020**, *142* (41), 17589-17597. DOI: 10.1021/jacs.0c07763.
(34) Brar, A.; Wang, X. S.; Gillis, C. N.; Yang, J. Y.; Findlater, M. Challenges in Product Selectivity for Electrocatalytic Reduction of Amine-Captured CO2: Implications for Reactive Carbon Capture. *ACS Omega* **2025**, *10* (21), 21980-21984. DOI: 10.1021/acsomega.5c02049.
(35) Wu, Y.; Rudshteyn, B.; Zhanaidarova, A.; Froehlich, J. D.; Ding, W.; Kubiak, C. P.; Batista, V. S. Electrode-Ligand Interactions Dramatically Enhance CO2 Conversion to CO by the [Ni(cyclam)](PF6)2 Catalyst. *ACS Catalysis* **2017**, *7* (8), 5282-5288. DOI: 10.1021/acscatal.7b01109.

(36) Froehlich, J. D.; Kubiak, C. P. Homogeneous CO2 Reduction by Ni(cyclam) at a Glassy Carbon Electrode. *Inorg. Chem.* **2012**, *51* (7), 3932-3934. DOI: 10.1021/ic3001619.
(37) Kelly, C. A.; Blinn, E. L.; Camaioni, N.; D'Angelantonio, M.; Mulazzani, Q. G. Mechanism of CO2 and H+ Reduction by Ni(cyclam)+ in Aqueous Solution. A Pulse and Continuous Radiolysis Study. *Inorg. Chem.* **1999**, *38* (7), 1579-1584. DOI: 10.1021/ic980902p.
(38) Kelly, C. A.; Mulazzani, Q. G.; Venturi, M.; Blinn, E. L.; Rodgers, M. A. J. The Thermodynamics and Kinetics of CO2 and H+ Binding to Ni(cyclam)+ in Aqueous Solution. *J. Am. Chem. Soc.* **1995**, *117* (17), 4911-4919. DOI: 10.1021/ja00122a023.
(39) Fujihira, M.; Hirata, Y.; Suga, K. Electrocatalytic reduction of CO2 by nickel(II) cyclam: Study of the reduction mechanism on mercury by cyclic voltammetry, polarography and electrocapillarity. *Journal of Electroanalytical Chemistry and Interfacial Electrochemistry* **1990**, *292* (1), 199-215. DOI: https://doi.org/10.1016/0022-0728(90)87336-I.
(40) Beley, M.; Collin, J. P.; Ruppert, R.; Sauvage, J. P. Electrocatalytic reduction of carbon dioxide by nickel cyclam2+ in water: study of the factors affecting the efficiency and the selectivity of the process. *J. Am. Chem. Soc.* **1986**, *108* (24), 7461-7467. DOI: 10.1021/ja00284a003.
(41) Beley, M.; Collin, J.-P.; Ruppert, R.; Sauvage, J.-P. Nickel(II)-cyclam: an extremely selective electrocatalyst for reduction of CO2 in water. *J. Chem. Soc., Chem. Commun.* **1984**, (19), 1315-1316, 10.1039/C39840001315. DOI: 10.1039/C39840001315.
(42) Schneider, C. R.; Lewis, L. C.; Shafaat, H. S. The good, the neutral, and the positive: buffer identity impacts CO2 reduction activity by nickel(ii) cyclam. *Dalton Trans.* **2019**, *48* (42), 15810-15821, 10.1039/C9DT03114F. DOI: 10.1039/C9DT03114F.
(43) Neri, G.; Aldous, I. M.; Walsh, J. J.; Hardwick, L. J.; Cowan, A. J. A highly active nickel electrocatalyst shows excellent selectivity for CO2 reduction in acidic media. *Chemical Science* **2016**, *7* (2), 1521-1526, 10.1039/C5SC03225C. DOI: 10.1039/C5SC03225C.
(44) Song, J.; Klein, E. L.; Neese, F.; Ye, S. The Mechanism of Homogeneous CO2 Reduction by Ni(cyclam): Product Selectivity, Concerted Proton–Electron Transfer and C–O Bond Cleavage. *Inorg. Chem.* **2014**, *53* (14), 7500-7507. DOI: 10.1021/ic500829p.
(45) Forget, A.; Regnacq, M.; Orain, C.; Touzé, E.; Lelong, E.; Brandily, C.; Bernard, H.; Tripier, R.; Le Poul, N. Electrocatalytic reduction of CO2 in water by a C-functionalized Ni–cyclam complex grafted onto carbon. *Chemical Communications* **2022**, *58* (48), 6785-6788, 10.1039/D2CC01667B. DOI: 10.1039/D2CC01667B.
(46) Banerjee, A.; Yue, C.; Choi, J.; Morales-Guio, C. G. Rotating cylinder electrode in reactive CO2 capture: Identifying active C species via transport, VLE models and kinetics. *AIChE J.* **2024**, *70* (12), e18560. DOI: https://doi.org/10.1002/aic.18560.
(47) Shen, K.; Cheng, D.; Reyes-Lopez, E.; Jang, J.; Sautet, P.; Morales-Guio, C. G. On the origin of carbon sources in the electrochemical upgrade of CO2 from carbon capture solutions. *Joule* **2023**, *7* (6), 1260-1276. DOI: https://doi.org/10.1016/j.joule.2023.05.010.
(48) **!!! INVALID CITATION !!! 27, 31-34, 40, 41**.
(49) Peters, S. R. H., Jonathon O. A Controlled Growth Mercury Electrode. *Curr. Sep.* **1994**, *13*, 1-5.
(50) Kowalski, Z. Application of a controlled-growth mercury drop electrode to polarography. *Analyst* **1988**, *113* (1), 15-19.
(51) Balazs, G. B.; Anson, F. C. The adsorption of Ni(cyclam)+ at mercury electrodes and its relation to the electrocatalytic reduction of CO2. *J. Electroanal. Chem.* **1992**, *322* (1), 325-345. DOI: https://doi.org/10.1016/0022-0728(92)80086-J.
(52) Bujno, K.; Bilewicz, R.; Siegfried, L.; Kaden, T. A. Effects of ligand structure on the adsorption of nickel tetraazamacrocyclic complexes and electrocatalytic CO2 reduction. *J. Electroanal. Chem.* **1998**, *445* (1), 47-53. DOI: https://doi.org/10.1016/S0022-0728(97)00603-7.
(53) **!!! INVALID CITATION !!! 42-45**.
(54) **!!! INVALID CITATION !!! 10-12, 42, 46, 47**.
(55) Barzagli, F.; Giorgi, C.; Mani, F.; Peruzzini, M. Screening Study of Different Amine-Based Solutions as Sorbents for Direct CO2 Capture from Air. *ACS Sustainable Chemistry & Engineering* **2020**, *8* (37), 14013-14021. DOI: 10.1021/acssuschemeng.0c03800.
(56) Puxty, G.; Rowland, R.; Allport, A.; Yang, Q.; Bown, M.; Burns, R.; Maeder, M.; Attalla, M. Carbon Dioxide Postcombustion Capture: A Novel Screening Study of the Carbon Dioxide Absorption Performance of 76 Amines. *Environmental Science & Technology* **2009**, *43* (16), 6427-6433. DOI: 10.1021/es901376a.
(57) Sartori, G.; Savage, D. W. Sterically hindered amines for carbon dioxide removal from gases. *Industrial & Engineering Chemistry Fundamentals* **1983**, *22* (2), 239-249. DOI: 10.1021/i100010a016.
(58) Dell'Amico, D. B.; Calderazzo, F.; Labella, L.; Marchetti, F.; Pampaloni, G. Converting Carbon Dioxide into Carbamato Derivatives. *Chemical Reviews* **2003**, *103* (10), 3857-3898. DOI: 10.1021/cr940266m.
(59) Ma, C.; Pietrucci, F.; Andreoni, W. CO(2) Capture and Release in Amine Solutions: To What Extent Can Molecular Simulations Help Understand the Trends? *Molecules* **2023**, *28* (18). DOI: 10.3390/molecules28186447 From NLM.
(60) Versteeg, G. F.; J., V. D. L. A.; and Van Swaaij, W. P. M. ON THE KINETICS BETWEEN CO2 AND ALKANOLAMINES BOTH IN AQUEOUS AND NON-AQUEOUS SOLUTIONS. AN OVERVIEW. *Chem. Eng. Commun.* **1996**, *144* (1), 113-158. DOI: 10.1080/00986449608936450.
(61) McCann, N.; Phan, D.; Fernandes, D.; Maeder, M. A systematic investigation of carbamate stability constants by 1H NMR. *International Journal of Greenhouse Gas Control* **2011**, *5* (3), 396-400. DOI: https://doi.org/10.1016/j.ijggc.2010.01.008.
(62) Aytac, Y.; Yunus, K. Statistical Analysis of Substituent Effects on pKa of Aniline. *Journal of Engineering Research and Applied Science* **2024**, *13* (2). (acccessed 2025/05/06).
(63) Reyes-Ortega, F.; Parra-Ruiz, F. J.; Averick, S. E.; Rodríguez, G.; Aguilar, M. R.; Matyjaszewski, K.; San Román, J. Smart heparin-based bioconjugates synthesized by a combination of ATRP and click chemistry. *Polymer Chemistry* **2013**, *4* (9), 2800-2814, 10.1039/C3PY00055A. DOI: 10.1039/C3PY00055A.
(64) Hall, H. K., Jr. Correlation of the Base Strengths of Amines1. *J. Am. Chem. Soc.* **1957**, *79* (20), 5441-5444. DOI: 10.1021/ja01577a030.
(65) Zhang, Z.; Kummeth, A. L.; Yang, J. Y.; Alexandrova, A. N. Inverse molecular design of alkoxides and phenoxides for aqueous direct air capture of CO2. *Proceedings of the National Academy of Sciences* **2022**, *119* (25), e2123496119.
(66) 13C NMR spectra can be performed in a quantitative fashion. However, the long relaxation time for 13C nuclei requires extended collection times, which we were unable to obtain for all 12 samples used herein.
(67) Richner, G.; Puxty, G. Assessing the Chemical Speciation during CO2 Absorption by Aqueous Amines Using in Situ FTIR.

Ind. Eng. Chem. Res. **2012**, *51* (44), 14317-14324. DOI: 10.1021/ie302056f.
(68) Park, S. H.; Lee, K. B.; Hyun, J. C.; Kim, S. H. Correlation and Prediction of the Solubility of Carbon Dioxide in Aqueous Alkanolamine and Mixed Alkanolamine Solutions. *Ind. Eng. Chem. Res.* **2002**, *41* (6), 1658-1665. DOI: 10.1021/ie010252o.
(69) Jackson, P.; Beste, A.; Attalla, M. Insights into amine-based CO2 capture: an ab initio self-consistent reaction field investigation. *Struct. Chem.* **2011**, *22* (3), 537-549. DOI: 10.1007/s11224-010-9719-2.
(70) Yamada, H.; Shimizu, S.; Okabe, H.; Matsuzaki, Y.; Chowdhury, F. A.; Fujioka, Y. Prediction of the Basicity of Aqueous Amine Solutions and the Species Distribution in the Amine−H2O−CO2 System Using the COSMO-RS Method. *Ind. Eng. Chem. Res.* **2010**, *49* (5), 2449-2455. DOI: 10.1021/ie901185v.
(71) Nakao, S.; Yogo, K.; Goto, K.; Kai, T.; Yamada, H. *Advanced CO2 Capture Technologies: Absorption, Adsorption, and Membrane Separation Methods*; Springer, 2019.
(72) Ma, C.; Pietrucci, F.; Andreoni, W. Capturing CO2 in Monoethanolamine (MEA) Aqueous Solutions: Fingerprints of Carbamate Formation Assessed with First-Principles Simulations. *The Journal of Physical Chemistry Letters* **2014**, *5* (10), 1672-1677. DOI: 10.1021/jz5006253.
(73) Deguchi, H.; Kubota, Y.; Yagi, Y.; Mitani, I.; Imai, Y.; Tatsumi, M.; Watari, N.; Hirata, T.; Kameda, Y. Structure of Monoethanolamine and Diethanolamine Carbamates in Aqueous Solutions Determined by High-Energy X-ray Scattering. *Ind. Eng. Chem. Res.* **2010**, *49* (1), 6-13. DOI: 10.1021/ie9009556.
(74) Sakaki, S. Can carbon dioxide coordinate to a nickel(I) complex? An ab initio MO/SD-CI study. *J. Am. Chem. Soc.* **1990**, *112* (21), 7813-7814. DOI: 10.1021/ja00177a062.
(75) Schneider, J.; Jia, H.; Kobiro, K.; Cabelli, D. E.; Muckerman, J. T.; Fujita, E. Nickel(ii) macrocycles: highly efficient electrocatalysts for the selective reduction of CO2 to CO. *Energy & Environmental Science* **2012**, *5* (11), 9502-9510, 10.1039/C2EE22528J. DOI: 10.1039/C2EE22528J.